Acta Scientiarum
http://periodicos.uem.br/ojs
ISSN on-line: 1807-8664
Doi: 10.4025/actascitechnol.v45i1.60443

Adsorption of food dye using activated carbon from brewers' spent grains

Luiz Eduardo Nochi Castro[1,2], Rosana Rabelo Mançano[1*], Débora Alessandra Jones Battocchio[1] and Leda Maria Saragiotto Colpini[1,2,3]

[1]Universidade Federal do Paraná, Rua Doutor João Maximiano, 426, 86900-000, Jandaia do Sul, Paraná, Brazil. [2]Programa de Pós-Graduação em Biotecnologia, Universidade Federal do Paraná, Palotina, Paraná, Brazil. [3]Programa de Pós-Graduação em Engenharia e Tecnologia Ambiental, Universidade Federal do Paraná, Palotina, Paraná, Brazil. *Author for correspondence. E-mail: rosanarabelo1313@gmail.com

ABSTRACT. Brewers' spent grains are the main residue generated from the brewery industry; they are produced on a large scale and at a low cost. During the brewing process, approximately 85% of all barley used is transformed into solid residue, which is currently destined for animal feed or just discarded. A possibility to increase the value of this byproduct is the production of carbonaceous materials, such as activated carbon, for the treatment of tartrazine yellow dye solutions. The structures and morphologies of the samples were characterized. Furthermore, the adsorptive capacity and kinetic behavior were studied. Regarding the characterization of the material, the activated carbon presented a porous morphology and high surface area (768.4 m^2 g^{-1}). Additionally, the kinetic study showed that the equilibrium time of the adsorption process from the tartrazine yellow dye discoloration was 60 min., and the data presented dispersion according to Elovich's kinetics. It was possible, from the experimental design, to evaluate the adsorptive capacity of the material in which it performed best at pH < 5. Finally, in the equilibrium study carried out by the adsorption isotherms, it was found that the increase in temperature influenced the process, raising the maximum adsorptive capacity in which the data fit into the Langmuir isothermal model.

Keywords: adsorbent; biomass; characterization; tartrazine yellow.

Received on August 4, 2021.
Accepted on April 4, 2022.

Introduction

Brewers' spent grains (BSG) are the residue that is produced during beer industrialization (Castro, Meurer, & Colpini, 2021), and it is produced on a large scale at a low cost (Mussatto, Dragone, & Roberto, 2006). Approximately 85% of all residues that come from beer production correspond to BSG, which is currently used for animal feed or simply is thrown away (Castro et al., 2021; Sganzerla et al., 2021a). In the beer production system, for every 100 L of beer produced, approximately 20 kg of BSG is generated (Sganzerla, Ampese, Mussatto, & Forster-Carneiro, 2021b). According to MAPA data, in 2018, Brazil produced approximately 14 billion liters of beer, which generated approximately 3 million tons of BSG (Brasil, 2020).

Due to the high amount of byproduct, its disposal may become problematic and often harmful to the environment if it is disposed of incorrectly. Moreover, the storage of this byproduct is usually impracticable, especially in large industries with a very high generation flow that do not have enough space or warehouses to store the residue. Even though it is used as animal feed, the amount generated exceeds the amount consumed. Therefore, it is necessary to find possible applications for the use of BSG, whether in nutritional applications for humans and/or animals, for energy generation or as a source for adsorbent production (Nocente, Taddei, Galassi, & Gazza, 2019; Castro & Colpini, 2021; Sganzerla, Buller, Mussatto, & Forster-Carneiro, 2021c).

Overall, BSG has the characteristics necessary to serve as a good adsorbent, such as a high concentration of minerals, especially carbon, silicon and aluminum, and a high volatile content, which helps generate a rich pore structure (Lam et al., 2018; Castro & Colpini, 2021). This means that extremely efficient and low-cost adsorbent materials can be obtained once the raw material is a residue and can easily be turned into activated carbon (Guimarães, Teixeira, Oliveira, & Lopes, 2020).

Chemical activation with nitric acid, phosphoric acid, potassium hydroxide, potassium carbonate, or physical activation with steam, carbon dioxide, ozone, and other procedures and techniques can be used to

activate carbon-based materials (Pongkua, Dolphen, & Thiravetyan, 2019; Duan, Yuan, Jing, & Yuan, 2019). Some factors, such as the cost and time spent synthesizing the material, the required equipment, the degree of difficulty of the synthesis, the type of reagent used and its toxicity, and, most importantly, the characteristics of the material produced, must be considered before selecting an activation method (Taer, Apriwandi, Taslim, Malik, & Usman, 2019; Son & Park, 2020).

In light of these considerations, chemical activation emerges as a promising option since it produces materials with a high micropore content and large surface area, which can be employed for the adsorption of high molecular weight species such as azo dyes. Furthermore, most reagents are nontoxic, and activation takes place in a short reaction time and at a low temperature of 300-400°C, which optimizes the synthesis process while lowering energy and personnel expenses. Furthermore, the reagents required are frequently inexpensive, lowering the overall cost of the operation (Olsson & Salmen, 1997; Ahmed et al., 2019).

Primary treatments, including coagulation, flocculation, and sedimentation, are commonly employed to treat liquid industrial effluents, and these treatments are well known and well studied in the literature (Fagnani, Alves, Castro, Kunh, & Colpini, 2019; Castro et al., 2020). However, they require large building areas, are used to treat large volumes of effluent, and as a result, use much material to treat the effluent and generate much sludge that needs to be treated (Chowdhury, Mostafa, Biswas, & Saha, 2013). Furthermore, they are frequently unable to remove the molecules responsible for the effluents' color, such as dye molecules, necessitating further treatment processes, increasing the process's time and expense (Dotto & McKay, 2020).

The adsorption process has been shown to be efficient, simple to operate, low in operational cost, zero sludge production, no chemical requirement, and extremely competent in discoloration and degradation processes, in addition to being able to reuse industrial waste in the form of activated carbon, becoming an alternative to traditional waste treatment methods (Barakan & Aghazadeh, 2021).

Their use in the adsorption of industrial effluents, particularly from the food industry, has been studied in recent years in the literature, and the results are generally better than those of other processes, making activated carbon adsorption an emerging technology that the industry may begin to adopt for the treatment of its liquid waste (Azmi & Yunos, 2014; Castro, Santos, Fagnani, Alves, & Colpini, 2019).

Therefore, the main goal of this work was to evaluate the use of BSG to produce activated carbon (AC) in the adsorption of tartrazine yellow dye solution (TY).

Materials and methods

Collection and preparation of samples

The samples of BSG (approximately 10 kg) were provided by a company that produces fermented beverages in the region of Vale do Ivaí, in the state of Paraná, Brazil, and immediately stored after collection at 4°C until use. Previously, the BSG samples were quartered until there was a visual reduction of 80% from the initial mass. Then, the quartered samples were washed in running water until the residual liquid did not show any colors. Posteriorly, they were stored in plastic bags, vacuum sealed, labeled *in natura* and frozen until use to avoid any kind of possible contamination by microbiological agents. The sample portion intended for the production of adsorbents was dried in a natural convection oven at a temperature of 90°C for 12 hours and then stored in plastic bags, vacuum sealed, and frozen until further analysis was performed.

Preliminary test of adsorptive capacity

To evaluate whether the characteristics presented by the BSG were ideal to obtain a good adsorbent, a discoloration test was performed with the TY food dye solutions. Fifty milliliters of dye solution with a concentration of 10 mg L^{-1} was added to 500 mg of dry BSG and stirred in a shaker incubator for 12 hours at room temperature. At the end of the process, the mixture was filtered, where the absorbance of the dye was measured in a UV/Vis spectrophotometer at the maximum wavelength, $\lambda_{máx}$ = 427 nm, and the removal percentage was determined by Equation 1.

$$\%R = \left(\frac{C_0 - C_t}{C_0}\right) * 100 \quad (1)$$

where:

%R is the removal percentage (discoloring) of the TY dye, C_0 is the TY dye solution initial concentration (mg L^{-1}), and C_t is the TY dye solution concentration at time t (mg L^{-1}).

Adsorbent preparation

To improve the adsorptive capacity of BSG, the production of AC was performed using two different activation techniques to determine which technique would have the best performance for the adsorption of the TY dye. Precursor preparation, chemical activation and carbonization procedures were established based on preliminary tests and on literature data about AC production by chemical activation of agro-industrial residues (Namane, Mekarzia, Benrachedi, Belhaneche-Bensemra, & Hellal, 2005; Patnukao & Pavasant, 2008; Srihari & Das, 2008).

Chemical activation using phosphoric acid (H_3PO_4)

The washed and dried BSG were subjected to chemical activation using a desiccant precursor and subsequent carbonization, following the adapted methodology from Patnukao and Pavasant (2008). A phosphoric acid solution (85%) was added to the precursor material at a ratio of 1:1 (m v^{-1}) and manually stirred for approximately 3 min. at room temperature. Afterwards, the mixture was washed with distilled water to remove any excess acid and carbonized in porcelain crucibles. Carbonization was performed in a muffle furnace with a heating ramp (10°C $min.^{-1}$) up to 400°C for 5 hours. Later, the AC was labeled as P.A.A.C.

Chemical activation using hydrogen peroxide (H_2O_2)

The washed and dried BSG were subjected to chemical activation using an oxidizing precursor and subsequent carbonization, according to the adapted methodology from Moreno-Castilla et al. (1995). A hydrogen peroxide solution (30%) was added to the precursor material at a ratio of 1:2 (m v^{-1}), manually stirred for approximately 5 min. and kept in an ultrasonic bath for 20 min.. Thereafter, the mixture was washed with distilled water to remove any excess peroxide and carbonized in porcelain crucibles. Carbonization was also carried out in a muffle furnace with a heating ramp (10°C $min.^{-1}$) up to 400°C for 5 hours, and the AC was labeled H.P.A.C.

Morphological, structural and surface characterization

The morphology, structure and surface of BSG were studied using the following techniques: (1) scanning electron microscopy (SEM) with energy X-ray dispersive spectroscopy (EDS); (2) physisorption of N_2; (3) Fourier transform infrared spectroscopy (NIR/FTIR); and (4) point of zero charge (pH_{PZC}). SEM/EDS was performed using a VEGA3 model from TESCAN. The determination of specific surface area (S_o), average pore volume (V_p) and average pore diameter (d_p) were performed by physisorption of N_2 measurements using model NOVA 2000e equipment from Quantachrome Instruments. Therefore, the V_p and d_p values were determined by the Brunauer, Emmett and Teller method (B.E.T.). FTIR was carried out using a BRUKER – TENSOR 37 spectrophotometer with a Fourier transform and integrating sphere for diffuse reflectance analysis in an NIR ratio of 9,500 to 4,000 cm^{-1} with a resolution of 4 cm^{-1} and accumulating 128 duplicate scans. Last, pH_{PZC} was performed in a shaker incubator according to the Castro et al (2019) methodology.

Adsorption preliminary tests

Tests with different activation methods

To evaluate which activation method provided the greatest increase in the percentage of TY dye removal, an identical test to the one presented in the preliminary test of adsorptive capacity was performed using the adsorbents P.A.A.C and H.P.A.C.

Tests with different concentrations of adsorbent

After determining which AC provided the greatest percentage of TY dye removal, it was determined which concentration of the chosen adsorbent would have the best adsorptive capacity. For that matter, the activated carbon concentration was varied to 1, 2, 3, 4, 5 and 10 g L^{-1}, which were added to 50 mL of TY dye solution with a concentration of 10 mg L^{-1} in a similar procedure to the one presented in the adsorptive capacity preliminary test.

AT dye adsorption study

Adsorption kinetics study

To determine the equilibrium time (t_e) for the adsorption tests, the kinetic study was carried out with 50 mL of TY dye at a concentration of 10 mg L^{-1}, in which the adsorbent was added at a concentration of 2 g L^{-1}.

Aliquots were collected at reaction times of 1, 5, and 10 min. and at intervals of 15 min. until 135 min., and the amount of adsorbed dye (q_t) in the adsorbent phase was determined using Equation 2.

$$q_t = \left(\frac{C_0 - C_e}{m}\right) * V \quad (2)$$

where:

q_t is the amount of adsorbed TY dye (mg of dye g^{-1} of adsorbent), C_e is the TY dye concentration at equilibrium (mg L^{-1}), V (L) is the TY dye solution volume, and m is the adsorbent mass (g).

Then, the theoretical amount of TY dye adsorbed at equilibrium (q_e) was determined following three kinetic models: pseudofirst order model, pseudosecond order and Elovich; thereafter, they were compared to the experimental value of the amount of TY dye adsorbed at equilibrium (q_{eExp}). Additionally, the TY dye diffusion mechanism was investigated using the intraparticle diffusion model; all equations are shown in Table 1.

Table 1. Kinetic models used in the experiment.

Model	Equation	Reference
Pseudofirst order	$q_t = q_e(1-e^{-k_1 t})$	Lagergren (1898)
Pseudosecond order	$q_t = \frac{k_2 q_e^2 t}{1+(k_2 q_e t)}$ $h = k_2 q_e^2$	Ho and McKay (1998)
Elovich	$q_t = \frac{1}{\beta} \ln(\alpha\beta t)$	Low (1960)
Intraparticle diffusion	$q_t = (k_{ip}\, t^{0,5}) + C$	Ruthven (1984)

Where qt is the amount of adsorbed TY dye (mg of dye g^{-1} of adsorbent); q_e = adsorbed amount at equilibrium per unit mass of adsorbent (mg g^{-1}); k_1 = pseudofirst order adsorption kinetic constant ($min.^{-1}$); t= reaction time (min.); k_2 = pseudosecond order adsorption kinetic constant (g mg^{-1} $min.^{-1}$); h = initial adsorption rate (mg g^{-1} $min.^{-1}$); β = desorption constant (g mg^{-1}); α= initial adsorptive rate (mg g^{-1} $min.^{-1}$); k_{ip} = intraparticle diffusion rate (mg g^{-1} $min.^{-0,5}$); and C= constant of the intraparticle diffusion model.

Experimental design

To optimize the experiment and increase the AC adsorption capacity, a 2^2 factorial design was performed with repetition at the center point where the influence of pH and reaction temperature under the response variable, q_t, was evaluated. The levels studied and experimental tests are shown in Table 2.

The results obtained from the experimental design for the adsorption tests were put under statistical analysis using a significance level of α = 0.05, in which the effect of the factors and the interaction were statistically tested through analysis of variance (ANOVA) at STATITICA 7 (StatSoft).

Table 2. Control variables considered in the 2^2 factorial design.

Variable	Low level (-1)	Center point (0)	High level (+1)
Temperature (°C)	20	30	40
pH	3	7	11

Adsorption isotherm study

The existence of the TY dye equilibrium between the liquid and solid phases was studied through adsorption isotherms. The experimental isotherm data were collected at different temperatures of 25, 35 and 45°C and subsequently adjusted using the Langmuir and Freundlich models. The parameters and equations are shown in Table 3.

Table 3. Models of isotherms used in the experiment.

Model	Equation	Reference
Langmuir	$q_e = \frac{q_m k_L C_e}{1+(k_L C_e)}$ $R_L = \frac{1}{1+(k_L C_m)}$	Langmuir (1916)
Freundlich	$q_e = k_F \left(C_e^{\frac{1}{n}}\right)$	Freundlich (1906)

Where q_e = adsorbed amount at equilibrium per unit mass of adsorbent (mg g^{-1}); Ce was the TY dye concentration at equilibrium (mg L^{-1}); q_m = maximum amount adsorbed per mass unit of adsorbent (mg g^{-1}); k_L = constant related to the adsorption capacity of the Langmuir model (L mg^{-1}); R_L =Langmuir isotherm separation factor (dimensionless); C_m= maximum initial concentration (mg L^{-1}); k_F = constant related to the adsorption capacity of the Freundlich model (L mg^{-1}); and n = exponential Freundlich constant representing the parameter that characterizes the quasi-Gaussian energetic heterogeneity of the adsorption surface (dimensionless).

Results and discussion

Characterization of BSG and adsorbents

Scanning electron microscopy (SEM)

Figure 1 displays the results obtained through scanning electron microscopy of BSG and the P.A.A.C and H.P.A. C adsorbents.

It was possible to observe that all materials have pores on their surface, with special attention to Figure 1b, in which the material presented a high pore distribution all over the surface, an extremely important factor in the adsorption process, since the dye molecules find high numbers of active sites on the surface of the adsorbent to be adsorbed. Other studies in the literature have reported this behavior (Silva et al., 2004; Vanreppelen et al., 2014; Castro et al., 2019). Table 4 shows the results obtained through the EDS analysis.

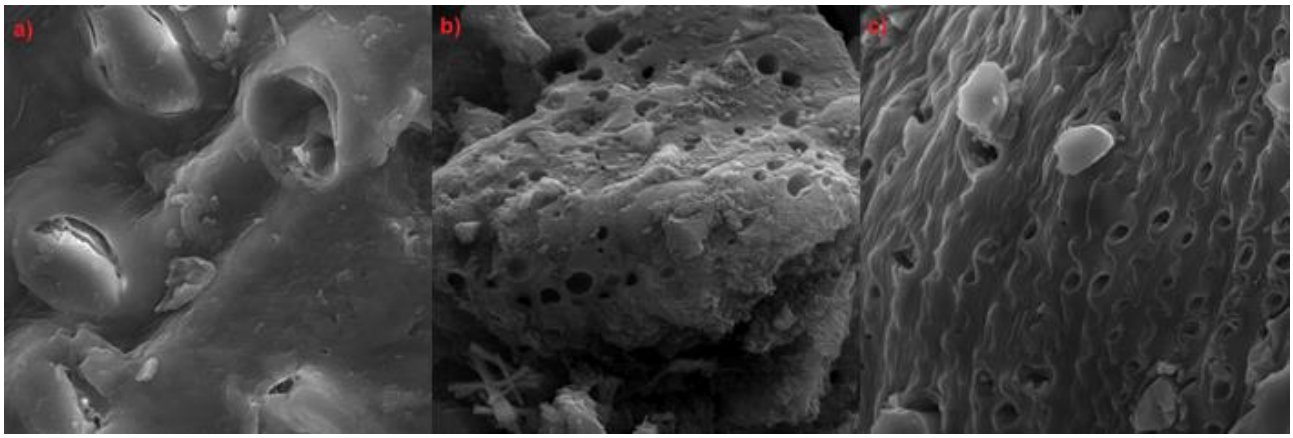

Figure 1. Scanning electron micrographs of materials at a magnification of 5,000x: a) BSG; b) P.A.A. C; c) H.P.A.C

Table 4. Elemental analysis by EDS.

Sample	Element (%)								
	Carbon (C)	Oxygen (O)	Silicon (Si)	Magnesium (Mg)	Potassium (K)	Calcium (Ca)	Aluminum (Al)	Phosphor (P)	Nitrogen (N)
BSG	65.13	33.64	0.12	0.26	0.11	0.74	-	-	-
P.A.A.C	77.93	17.27	0.35	-	-	-	0.05	4.40	-
H.P.A.C	36.45	35.82	2.30	0.77	-	0.70	-	-	21.10

It was possible to observe that for the BSG sample, the major element was carbon with approximately 65.13%, followed by oxygen with approximately 33.64%. It was expected that these compounds would appear in greater amounts, since the major components of BSG are carbohydrates. The elements in lower amounts, such as silicon, magnesium, potassium and calcium, come from the nature of the barley grain used for malt production.

In general, carbon was the element that appeared in greater quantity in the synthesized materials, indicating that a carbonization process occurred during the synthesis; the high carbon content may also indicate that the material has adsorptive capacity (Castro et al., 2019). The presence of oxygen was also expected since during the burning process, the materials were exposed to oxygen from the environment. The presence of phosphorus in the P.A.A.C sample came from phosphoric acid (H_3PO_4) used during the synthesis.

Physisorption measurements of N_2

The obtained isotherms are shown in Figure 2. It was observed that the isotherm from the P.A.A.C adsorbent is similar to the type IV isotherm, typical of mesoporous materials ($20 < d_p < 500$ Å). The hysteresis phenomenon that these isotherms show is caused by capillary condensation, which also confirms the presence of a mesoporous structure of the material. In addition, the '*gap*' from the hysteresis is an H2 type, with ink bottle-shaped pores, according to IUPAC (Deshmane, Owen, Abrokwah, & Kuila, 2015; Gao, Wang, Zhang, Guo, & Zhang, 2016; Hashemi-Uderji, Abdollahi-Alibeik, & Ranjbar-Karimi, 2018). The isotherms from BSG and P.A.A.C. adsorbents were similar to type II isotherms, typical of nonporous or macroporous materials, according to IUPAC (Castro et al., 2019).

These results corroborate the micrographs shown in Figure 2, in which the surfaces of materials (a) and (c) have fewer pores, and material (b) has a high number of pores, which can be confirmed by the values shown in Table 5.

From Table 5, it was observed that the P.A.A.C adsorbent has the largest surface area of approximately 770 $m^2\ g^{-1}$, while the other adsorbents have substantially smaller values. Zhang and Wang (2016) found surface area values of 17.53 to 223.08 $m^2\ g^{-1}$ when they used BSG biochar. However, Mussatto et al. (2010) found surface area values for AC of BSG ranging between 33 and 692 $m^2\ g^{-1}$.

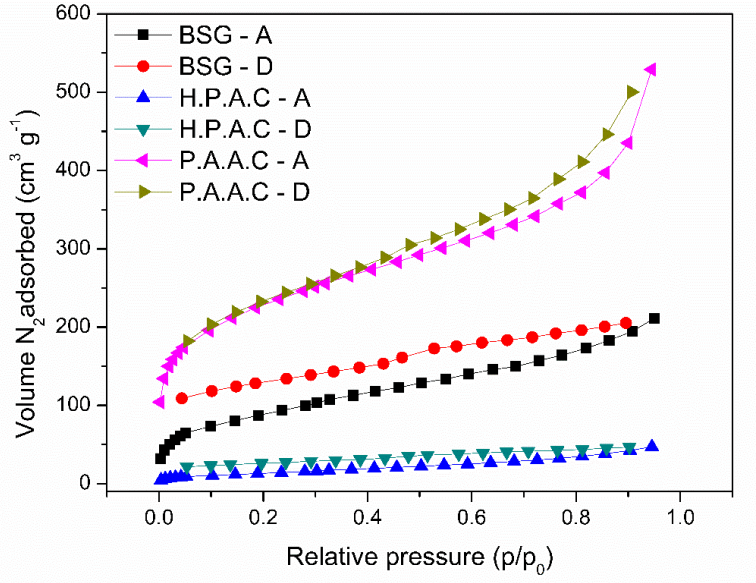

Figure 2. Adsorption (A) and desorption (D) isotherms of N_2 in the materials.

Table 5. Surface area (S_0), average pore volume (V_P) and average pore diameter (d_P) for the analyzed materials.

Sample	S_0 ($m^2\ g^{-1}$)	V_p ($cm^3\ g^{-1}$)	d_p (Å)
BSG	104.30	0.11	20.30
P.A.A.C	768.40	0.82	21.00
H.P.A.C	165.80	0.02	28.04

Fourier transform infrared spectroscopy (FTIR)

The FTIR spectra of BSG and the activated carbons are shown in Figure 3.

It was possible to observe from the NIR spectra of Figure 3a three regions where signs of compounds present in the BSG were found. In region 1, which comprises wavelengths from 8,000 to 8,750 cm^{-1}, it was possible to identify characteristic vibration signals of the $-CH_3$, $-CH_2$ and -CH bonds in the second overtone region. In region 2, which consists of the spectra of the wavelengths from 6,000 to 7,500 cm^{-1}, the same vibrations were observed, which may indicate a possible presence of cellulosic compounds such as hemicellulose, lignin and cellulose (McLellan, Aber, Martin, Melillo, & Nadelhoffer, 1991; Li, Sun, Zhou, & He, 2015). For region 3, which comprises 4,500 to 5,400 cm^{-1}, it was possible to identify vibration characteristics between –C-C and H_2O bonds in the combination region (Xiaobo, Jiewena, Povey, Holmes, & Hanpin, 2010).

Figure 3b shows that the spectra presented a completely different structure from BSG, possibly due to the surface change caused by chemical activation. However, it was not possible to identify characteristic vibrations of bounds since the analytical signal is basically composed of noise, which may be a result of the surface change of the material, making it difficult to carry out the analysis. Most likely, a medium infrared analysis would be able to identify compounds in the adsorbents, as reported in other works in the literature (Haddad, Mamouni, Saffaj, & Lazar, 2012; Ferraz, Amorim, Tavares, & Teixeira, 2015).

Point of zero charge (pH_{ZPC})

From the pH_{PZC} analysis, the data from Figure 4 were obtained and show the pH_{PZC} values of the samples. The pH value for the TY dye solution at a concentration of 10 mg L^{-1} was approximately 6.6.

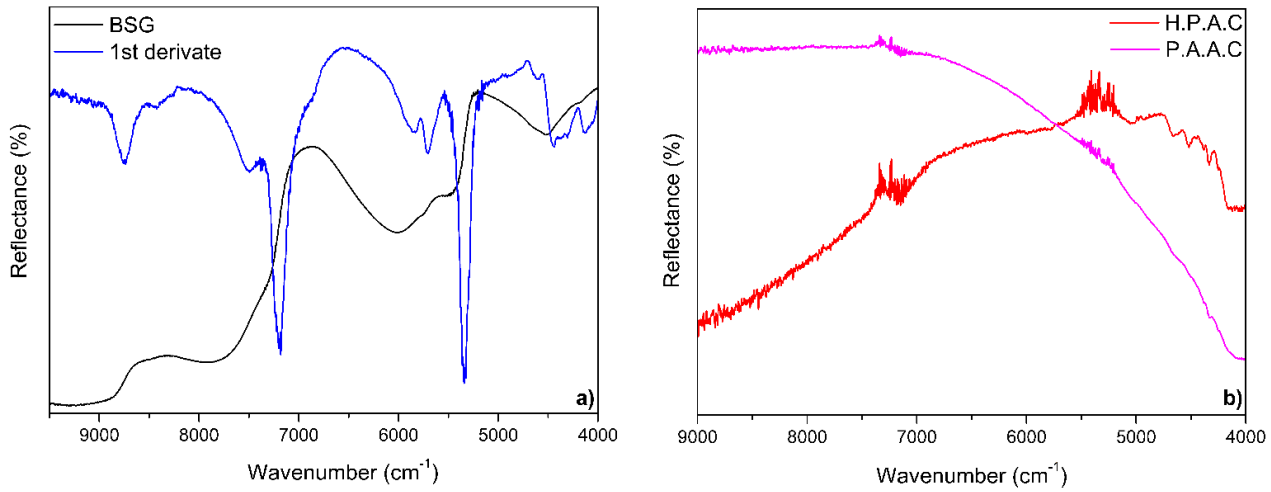

Figure 3. Infrared spectra in the NIR region: a) BSG and b) activated carbons.

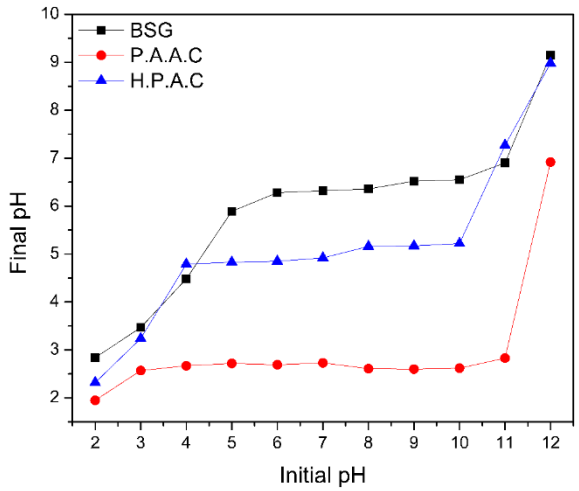

Sample	pH_{PCZ}
BSG	6.41
P.A.A.C	2.66
H.P.A.C	4.99

Figure 4. Determination of the point of zero change from the samples.

The main objective of the point of zero charge (pH_{PZC}) was to evaluate the surface behavior of an adsorbent material in an aqueous medium, where the tendency of the material surface for acidity or basicity can be inferred, indicating whether it is negatively or positively charged when in a medium in which the pH is higher or lower than its pH_{PZC}, respectively (Merg et al., 2010; Castro et al., 2019).

It was possible to observe that the pH value for all materials is below the pH of the dye solution; therefore, the surface of the adsorbents is positively charged, which leads to the attraction of negatively charged species. It is known that dye molecules have free electrons in their structure (Lee, Shim, Yang, Choi, & Jeon, 2019), and there is a tendency to have a negative charge, which helps in the adsorption process onto positive surfaces, as in the adsorbents in this study.

Adsorption preliminary tests

Regarding the preliminary adsorption test, it was possible to obtain the block graph shown in Figure 5.

Figure 5a shows that the material treated with H_3PO_4 removed approximately 75% of the TY dye, while the one treated with H_2O_2 removed approximately 45%, a removal rate lower than that with phosphoric acid treatment. Silva et al. (2004) obtained a removal > 90% of the acid orange dye 7 when they used BSG activated carbon as an adsorbent. Jaikumar and Ramamurthi (2009) completely removed acid yellow dye 17 from aqueous solutions at a 25 mg L^{-1} concentration when they used BSG grains treated with sulfuric acid. These data indicate that BSG can be used effectively to produce activated carbons in dye adsorption tests.

The difference in removal of the TY dye is explained by the characterization of the material. It was possible to observe from the pH_{PZC} analysis that all materials had their surface positively charged, which provides for adsorption of anionic molecules, such as the dye molecules. However, since all materials had similar behavior,

other characteristics were decisive for the superior performance of activated carbon with phosphoric acid. From the micrographs and N_2 physisorption analysis, it was possible to observe that the structure and surface of the adsorbent treated with phosphoric acid was one of the reasons for the high removal of the TY dye from the solutions, as the material is highly porous and has a high surface area and presence of mesopores. For the material activated by H_2O_2, its structural characteristics, low surface area and low number of pores, did not favor it during the effluent adsorption process.

Therefore, it was chosen to use AC treated with phosphoric acid, as it showed the best results in the preliminary tests, in addition to having the characteristics for a good adsorbent material. To optimize the adsorbent usage, a concentration test was carried out to determine the lowest dose that the adsorbent would provoke the highest removal of the dye.

Figure 5b shows that the adsorbent concentration influenced the removal percentage. For the lowest concentration, 1 g L^{-1}, a discoloration of approximately 50% was obtained. For concentrations greater than or equal to 2 g L^{-1}, the removal of the TY dye was approximately 100%; for that reason, it was decided to use the minimum concentration that showed the best discoloration result, 2 g L^{-1}.

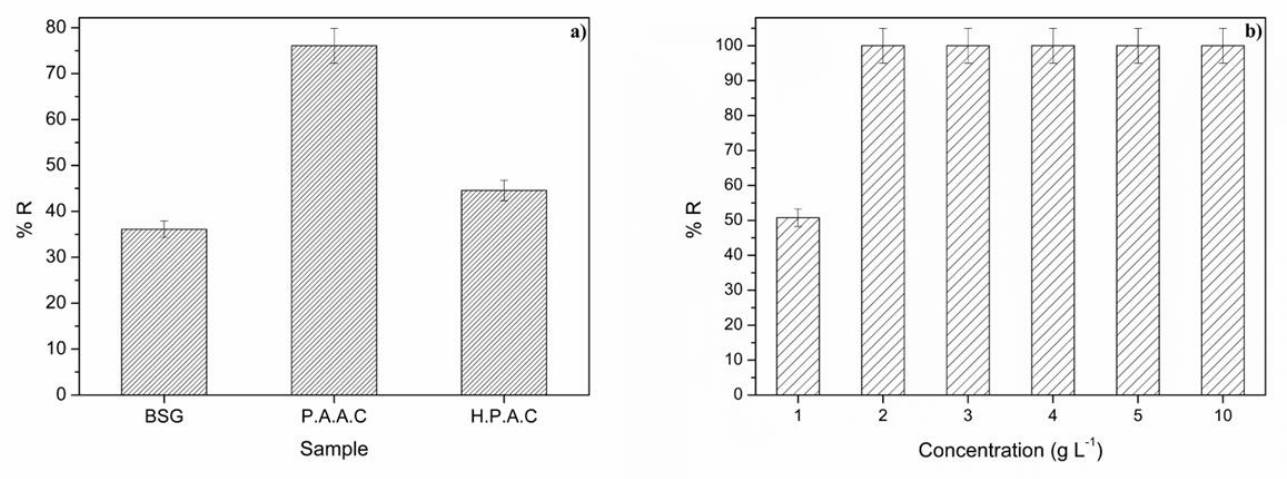

Figure 5. Results from the preliminary tests: a) different activation methods and b) adsorbent concentrations.

TY dye adsorption study

Adsorption kinetics

The adsorption kinetics of the TY dye and its applied models are shown in Figure 6, and its parameters are displayed in Table 6.

Figure 6a shows that the kinetic process of the dye was fast in the initial stages of the adsorption process, in which within 5 min., approximately 50% of the TY dye present in the solution was removed by the adsorbent. Additionally, it was observed that the kinetic equilibrium time for the experiment was 60 min.; from that moment, the amount of adsorbed dye remained the same. Therefore, the remainder of the experiment was carried out at conceptual equilibrium.

From Table 6, it was observed that the calculated values of q_e (calc) for both the first- and second-order models agreed with the experimental values of q_e (exp). The experimental data fit better to the pseudosecond order model (R^2 = 0.94 and RMSE = 0.39) than to the pseudofirst order model. Jaikumar and Ramamurthi (2009), Kezerle, Velić, Hasenay, and Kovačević (2018) and Silva et al. (2004) determined that the pseudosecond order model best fit the discoloration data for dyes yellow 17, Congo red, methylene blue and orange 7, respectively.

The Elovich model presented the best fit to the kinetic data of the TY dye among all models (R^2 = 0.98 and RMSE < 0.20), as it considers an exponential increase in the dye adsorption rate over time.

To perform a more complete evaluation of all kinetic behavior, it was possible to determine which mass flow stage rules the adsorption process through the study with the intraparticle diffusion model. According to Behnamfard and Salarirad (2009), when intraparticle diffusion is the main mechanism in the adsorption process, the q_e versus $t^{0,5}$ graph must be a straight line.

The intraparticle diffusion model for the adsorption of TY dye molecules on the P.A.A.C adsorbent is given in Figure 6b and illustrates that more than one process was involved in the adsorption process. The first stage (rapid removal, kip = 0.58 $min.^{-1}$) could be attributed to boundary layer diffusion, where the dye molecules

present in the liquid phase are transported to the solid surface of the adsorbent by external mass transfer factors, and the following equilibrium stage (slow removal, kip = 0.05 min.$^{-1}$) could be ascribed to the diffusion of TY dye molecules into the pores of the adsorbent (Khambhaty, Mody, Basha, & Jha, 2009).

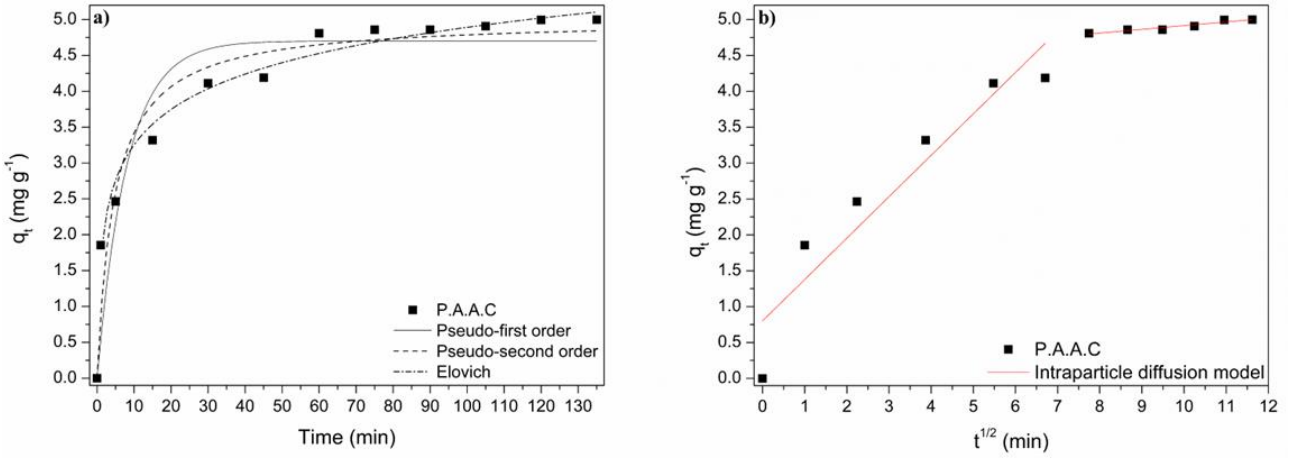

Figure 6. Adsorption kinetics of TY dye and models: a) First order, second order and Elovich; b) Intraparticle diffusion.

Table 6. Kinetic data modeling parameters.

Parameter	Pseudo-First Order	Pseudo-Second Order	Elovich	Intraparticle Diffusion[1,2]	
q_e (calc) (mg g^{-1})	4.70	5.01			
k_1	0.12	-	-		
k_2		0.04		-	
h		1.08			
α	-		6.91		
β		-	1.41		
k_{ip}			-	0.58	0.05
C				0.80	4.40
R^2	0.88	0.94	0.98	0.87	0.90
RMSE	0.54	0.39	0.18	0.09	0.11
q_e (exp) (mg g^{-1})		4.99			

Experimental design

The results of the adsorption tests performed based on the factorial design are shown in Table 7.

From the results observed in Table 7, it was possible to notice that assays 1 and 2, at pH = 3, obtained the highest values for qe, indicating a possible dependence on the pH of the reaction medium. To assess this dependence and the validity of the data obtained during the factorial experiment, statistical analysis was performed.

The results of the analysis of variance (ANOVA) of the tests showed a residual error of $\sqrt{0.212}$ = 0.46. Through ANOVA, it was also possible to observe that the pH of the reactional medium had a significant effect on the amount of dye removed from the solution, since the p value < 0.05. Figure 7 shows the main results of the statistical analysis of the experiment.

It was possible to note from the Pareto chart that Factor B – pH – was the one that had a statistically significant effect on the response variable, which confirms the information obtained by ANOVA. In Figure 7b, it was possible to observe that the temperature had nearly any significant effect on the q_t value, as the mean of q_t at the lowest level (20°C) was similar to that at the highest level (40°C). However, if the pH factor was considered, it had a significantly high impact on the amount of dye adsorbed; at the lowest pH, the value ranged approximately 17 mg g^{-1}, while at the highest pH, this value was approximately 8 mg g^{-1}, almost half the value. Since the main objective of statistical modeling is maximizing the value of q_t, the diagram indicates that it would be better to adjust the pH value to a lower level, as the downward slope expresses that the lower the pH is, the greater the amount of dye adsorbed by the adsorbent.

A first-order regression model with an adjusted regression coefficient (R_{adj}^2 = 0.988) was obtained and is shown in Equation 3.

$$y = 0.0214\, x_1x_2 - 1.836\, x_1 - 0.064\, x_2 + 31.67 \quad (3)$$

where:

y is the amount of tartrazine yellow dye adsorbed (mg g^{-1}), x_1 is the pH, and x_2 is the reaction temperature (°C).

Figure 7c presents the level curves obtained in the statistical analysis. The darker green region showed the highest values for the variable response, q_e, when the value of the y-axis (pH) was between 3 and 5, which indicates that the best adsorptive capacity occurs in an acid reaction medium. Moreover, Figure 7d shows the response surface obtained for the factorial design. The graph has a downward-facing concavity that resembles a first-degree equation curve.

Table 7. Factorial design results of TY dye adsorption tests.

Assay	Variable		q_e (mg g^{-1})
	Temperature (°C)	pH	
1	20	3	17.31
2	40	3	17.31
3	20	11	6.03
4	40	11	9.46
5	30	7	14.92
6	30	7	14.27
7	30	7	15.17

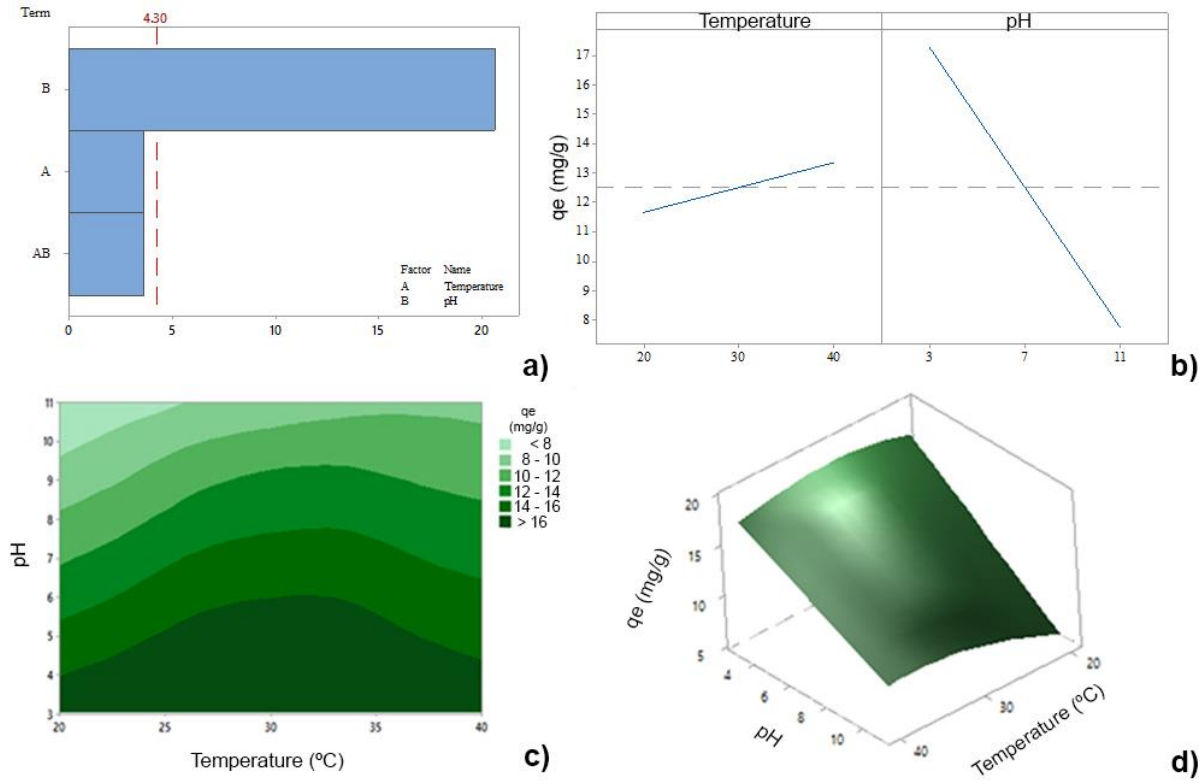

Figure 7. Statistical analysis of the experiment: a) Pareto chart, b) factor interaction diagram, c) level curves and d) response surface.

Adsorption isotherms

Regarding the adsorption isotherms and the data adjusted to the models, a dispersion graph was obtained, which can be seen in Figure 8.

Analyzing the adsorption isotherms shown in Figure 8, up to a concentration of 40 mg L^{-1}, the obtained format indicates a linear isotherm. At greater concentrations, the obtained format indicated favorable adsorption, and the increase in temperature from 25 to 35°C caused an increase in the adsorptive capacity of the adsorbents, which is natural to occur, since the temperature tends to favor the mass transfer process between the dye solution and the adsorbent (Behnamfard & Salarirad, 2009). However, when the temperature was increased to a value of 45°C, the amount of dye adsorbed decreased, which can be explained by the lower interaction between the adsorbent and the TY dye molecules at higher temperatures.

This decrease in the interaction may have occurred due to some steric impediment during the surface interaction between the dye molecules that are negatively charged with the molecules on the surface of the adsorbent; this steric effect acts as a barrier to the mass diffusion process between the compounds (Llorca et al., 2020; Santa-Cruz et al., 2021). Vasques, Souza, Weissenberg, Souza, and Valle (2011) obtained similar conclusions when utilizing residual sludge for the adsorption of R016, RR2 and RR141 dyes.

The parameters of the obtained isotherms are shown in Table 8.

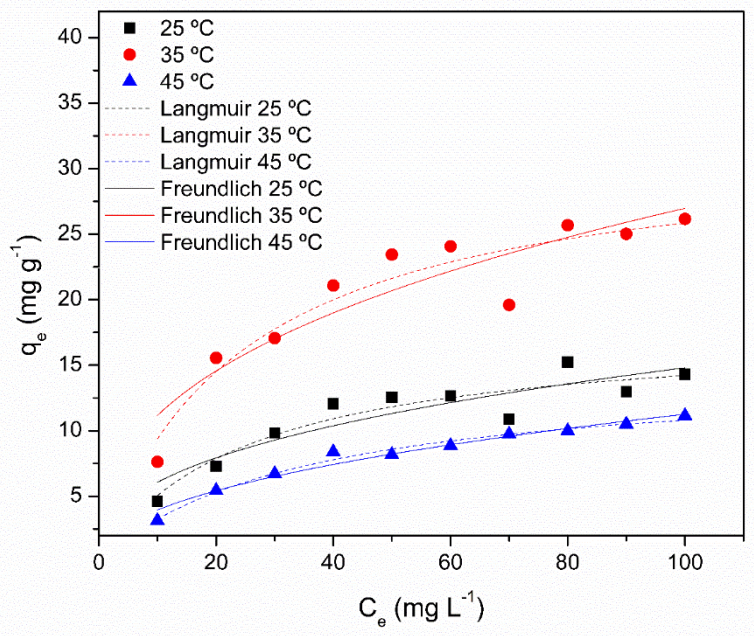

Figure 8. TY dye adsorption isotherms.

Table 8. Parameters of the Langmuir and Freundlich isotherm models.

Parameter	Langmuir			Freundlich		
	25°C	35°C	45°C	25°C	35°C	45°C
q_m	17.79	32.15	14.57			
k_L	0.04	0.04	0.03		-	
R_L	0.20	0.19	0.26			
k_F		-		2.48	4.62	1.39
n				2.58	2.61	2.20
R^2	0.87	0.89	0.98	0.81	0.83	0.93
RMSE	1.17	1.93	0.32	1.41	2.42	0.47

Comparing the coefficient of determination and the square root of the mean error of the Langmuir and Freundlich models, it was noted that the Langmuir isotherm was the best fit to the experimental data of the TY dye ($R^2 > 0.87$ and RMSE < 1.93) in the concentration analyzed.

The k_L parameter of the Langmuir model showed that by increasing temperature, there was a decrease in its value, which may indicate a possible decrease in the interaction between the TY dye and the adsorbent, which corroborates the data obtained in Figure 8, since it is related to the adsorption energy. The parameter 'n' of the Freundlich model indicated that for all temperatures, there was favorable adsorption (n > 1), a result that confirms the format presented by the isotherms. By analyzing the q_m parameter, it was noted that the maximum quantity of TY dye adsorbed by the adsorbent was at a temperature of 35°C (q_m = 32.15 mg g^{-1}), which indicates that the temperature of the process influences the adsorption process. The separation factor (R_L) of the Langmuir isotherm ranged from 0.19 to 0.26, showing that the adsorption of dye TY by the adsorbent is a thermodynamically favorable process.

Table 9 shows some results obtained in the literature for experiments similar to those obtained in this work. When compared to other precursors, BSG performs well as an activated carbon for TY dye adsorption. The BSG adsorbent in this work had a greater adsorption capacity (q_m) than other lignocellulosic materials in the literature. These findings suggest that BSG could be useful in the adsorption of dye molecules.

Table 9. Comparison of adsorption capacity from the literature.

Precursor	Dye	Experimental conditions		qm ($mg\ g^{-1}$)	Reference
		T (°C)	pH		
BSG	Tartrazine yellow	35	3	32.15	This study
BSG		30	2	26.18	Araújo, Tavares, Vareschini, and Barros (2020)
Sawdust		45	3	4.71	Banerjee and Chattopadhyaya (2017)
Deoiled soya		30	2	21.29	Mittal, Mittal, and Kurup (2006)
Cassava biomass		30	2	20.83	Chukwuemeka-Okorie, Ekuma, Akpomie, Nnaji, and Okereafor (2021)

Conclusion

It can be concluded that two types of BSG-based activated carbons were prepared using different methods of chemical activation. Through characterization analysis, all materials changed the initial characteristics of the raw material and somehow influenced its adsorptive capacity. P.A.A.C, presented the best performance in the adsorption tests, where approximately 100% of the dye molecules were removed from the solution, which shows that the objective of the work was successfully achieved since BSG can be used for the synthesis of activated carbons and these adsorbent materials are competent in environmental decontamination reactions of food dye effluents, such as tartrazine yellow food dye.

References

Ahmed, M. B., Johir, M. A. H., Zhou, J. L., Ngo, H. H., Nghiem, L. D., Richardson, C., ... Bryant, M. R. (2019). Activated carbon preparation from biomass feedstock: Clean production and carbon dioxide adsorption. *Journal of Cleaner Production, 225*, 405-413. DOI: https://doi.org/10.1016/j.jclepro.2019.03.342

Araújo, T. P., Tavares, F. O., Vareschini, D. T., & Barros, M. A. S. D. (2020). Biosorption mechanisms of cationic and anionic dyes in a low-cost residue from brewer's spent grain. *Environmental Technology, 42*(19), 2925-2940. DOI: https://doi.org/10.1080/09593330.2020.1718217

Azmi, N. S., & Yunos, K. F. (2014). Wastewater treatment of palm oil mill effluent (POME) by ultrafiltration membrane separation technique coupled with adsorption treatment as pre-treatment. *Agriculture and Agricultural Science Procedia, 2*, 257-264. DOI: https://doi.org/10.1016/j.aaspro.2014.11.037

Banerjee, S., & Chattopadhyaya, M. C. (2017). Adsorption characteristics for the removal of a toxic dye, tartrazine from aqueous solutions by a low cost agricultural by-product. *Arabian Journal of Chemistry, 10*(2), S1629-S1638. DOI: https://doi.org/10.1016/j.arabjc.2013.06.005

Barakan, S., & Aghazadeh, V. (2021). The advantages of clay mineral modification methods for enhancing adsorption efficiency in wastewater treatment: a review. *Environmental Science and Pollution Research, 28*, 2572-2599. DOI: https://doi.org/10.1007/s11356-020-10985-9

Behnamfard, A., & Salarirad, M. M. (2009). Equilibrium and kinetic studies on free cyanide adsorption from aqueous solution by activated carbon. *Journal of Hazardous Materials, 170*(1), 127-133. DOI: https://doi.org/10.1016/j.jhazmat.2009.04.124

Brasil. (2020). *Anuário da cerveja 2019*. Brasília, DF: Mapa.

Castro, L. E. N., & Colpini, L. M. S. (2021). All-around characterization of brewers' spent grain. *European Food Research and Technology, 247*, 3013-3021. DOI: https://doi.org/10.1007/s00217-021-03860-5

Castro, L. E. N., Meurer, E. C., Alves, H. J., Santos, M. A. R., Vasques, E. C., & Colpini, L. M. S. (2020). Photocatalytic degradation of textile dye orange-122 via electrospray mass spectrometry. *Brazilian Archives of Biology and Technology, 63*, e20180573. DOI: https://doi.org/10.1590/1678-4324-2020180573

Castro, L. E. N., Meurer, F., & Colpini, L. M. S. (2021). Estudo da aplicação de bagaço de malte como adsorvente para remoção de óleo lubrificante em meio aquoso. *Brazilian Journal of Development, 7*(12), 120522-120527. DOI: https://doi.org/10.34117/bjdv7n12-698

Castro, L. E. N., Santos, J. V. F., Fagnani, K. C., Alves, H. J., & Colpini, L. M. S. (2019). Evaluation of the effect of different treatment methods on sugarcane vinasse remediation. *Journal of Environmental Science and Health, 54*(9), 791-800. DOI: https://doi.org/10.1080/03601234.2019.1669981

Chowdhury, M., Mostafa, M. G., Biswas, T. K., & Saha, A. K. (2013). Treatment of leather industrial effluents by filtration and coagulation processes. *Water Resources and Industry, 3*, 11-22. DOI: https://doi.org/10.1016/j.wri.2013.05.002

Chukwuemeka-Okorie, H. O., Ekuma, F. K., Akpomie, K. G., Nnaji, J. C., & Okereafor, A. G. (2021). Adsorption of tartrazine and sunset yellow anionic dyes onto activated carbon derived from cassava sievate biomass. *Applied Water Sciences, 11*, 27. DOI: https://doi.org/10.1007/s13201-021-01357-w

Deshmane, V. G., Owen, S. L., Abrokwah, R. Y., & Kuila, D. (2015). Mesoporous nanocrystalline TiO_2 supported metal (Cu, Co, Ni, Pd, Zn, and Sn) catalysts: Effect of metal-support interactions on steam reforming of methanol. *Journal of Molecular Catalysis A: Chemical, 408*, 202-213. DOI: https://doi.org/10.1016/j.molcata.2015.07.023

Dotto, G. L., & McKay, G. (2020). Current scenario and challenges in adsorption for water treatment. *Journal of Environmental Chemical Engineering, 8*(4), 103988. DOI: https://doi.org/10.1016/j.jece.2020.103988

Duan, X.-L., Yuan, C.-G., Jing, T.-T., & Yuan, X.-D. (2019). Removal of elemental mercury using large surface area micro-porous corn cob activated carbon by zinc chloride activation. *Fuel, 239*, 830-840. DOI: https://doi.org/10.1016/j.fuel.2018.11.017

Fagnani, K. C., Alves, H. J., Castro, L. E. N., Kunh, S. S., & Colpini, L. M. S. (2019). An alternative for the energetic exploitation of sludge generated in the physico-chemical effluent treatment from poultry slaughter and processing in Brazilian industries. *Journal of Environmental Chemical Engineering, 7*(2), 102996. DOI: https://doi.org/10.1016/j.jece.2019.102996

Ferraz, A. I., Amorim, C., Tavares, T., & Teixeira, J. A. (2015). Chromium(III) biosorption onto spent grains residual from brewing industry: equilibrium, kinetics and column studies. *International Journal of Environmental Science and Technology, 12*, 1591-1602. DOI: https://doi.org/10.1007/s13762-014-0539-6

Freundlich, H. M. F. (1906). Over the adsorption in solution. *The Journal of Physical Chemistry, 57*, 385-471.

Gao, S., Wang, D., Zhang, P., Guo, X., & Zhang, X. (2016). Effects of process conditions on the structure and optical properties of Zn/Fe/Sn/Sb-TiO_2 three dimensional particle-electrodes. *Optik, 127*(16), 6519-6524. DOI: https://doi.org/10.1016/j.ijleo.2016.04.133

Guimarães, T., Teixeira, A. P. C., Oliveira, A. F., & Lopes, R. P. (2020). Biochars obtained from arabica coffee husks by a pyrolysis process: characterization and application in Fe(ii) removal in aqueous systems. *New Journal of Chemistry, 44*(8), 3310-3322. DOI: https://doi.org/10.1039/c9nj04144c

Haddad, M. E., Mamouni, R., Saffaj, N., & Lazar, S. (2012). Removal of a cationic dye – Basic Red 12 – from aqueous solution by adsorption onto animal bone meal. *Journal of the Association of Arab Universities for Basic and Applied Sciences, 12*(1), 48-54. DOI: https://doi.org/10.1016/j.jaubas.2012.04.003

Hashemi-Uderji, S., Abdollahi-Alibeik, M., & Ranjbar-Karimi, R. (2018). Fe_3O_4@FSM-16-SO_3H as a novel magnetically recoverable nanostructured catalyst: preparation, characterization and catalytic application. *Journal of Porous Materials, 26*, 467-480. DOI: https://doi.org/10.1007/s10934-018-0628-x

Ho, Y. S., & McKay, G. (1998). Sorption of dye from aqueous solution by peat. *Chemical Engineering Journal, 70*(2), 115-124. DOI: https://doi.org/10.1016/S0923-0467(98)00076-1

Jaikumar, V., & Ramamurthi, V. (2009). Biosorption of acid yellow by spent brewery grains in a batch system: equilibrium and kinetic modelling. *International Journal of Biology, 1*(1), 21-29. DOI: https://doi.org/10.5539/ijb.v1n1p21

Kezerle, A., Velić, N., Hasenay, D., & Kovačević, D. (2018). Lignocellulosic materials as dye adsorbents: adsorption of methylene blue and congo red on brewers' spent grain. *Croatica Chemica Acta, 91*(1), 53-64. DOI: https://doi.org/10.5562/cca3289

Khambhaty, Y., Mody, K., Basha, S., & Jha, B. (2009). Kinetics, equilibrium and thermodynamic studies on biosorption of hexavalent chromium by dead fungal biomass of marine *Aspergillus niger*. *Chemical Engineering Journal, 145*(3), 489-495. DOI: https://doi.org/10.1016/j.cej.2008.05.002

Lagergren, S. (1898). Zur theorie der sogenannten adsorption geloster stoffe. *Kungliga Svenska Vetenskapsakademiens, 24*, 1-39.

Lam, S. S., Su, M. H., Nam, W. L., Thoo, D. S., Ng, C. M., Liew, R. K., ... Vo, D. V. N. (2018). Microwave pyrolysis with steam activation in producing activated carbon for removal of herbicides in agricultural surface water. *Industrial Engineering Chemical Research, 58*(2), 695-703. DOI: https://doi.org/10.1021/acs.iecr.8b03319

Langmuir, I. (1916). The constitution and fundamental properties of solids and liquids. Part I. solids. *Journal of the American Chemical Society, 38*(11), 2221-2295. DOI: https://doi.org/10.1021/ja02268a002

Lee, S. Y., Shim, H. E., Yang, J. E., Choi, Y. J., & Jeon, J. (2019). Continuous flow removal of anionic dyes in water by chitosan-functionalized iron oxide nanoparticles incorporated in a dextran gel column. *Nanomaterials, 9*(8), 1164. DOI: https://doi.org/10.3390/nano9081164

Li, X., Sun, C., Zhou, B., & He, Y. (2015). Determination of Hemicellulose, Cellulose and Lignin in Moso Bamboo by Near Infrared Spectroscopy. *Scientific Reports, 5*, 17210. DOI: https://doi.org/10.1038/srep17210

Llorca, M., Ábalos, M., Vega-Herrera, A., Adrados, M. A., Abad, E., & Farré, M. (2020). Adsorption and desorption behaviour of polychlorinated biphenyls onto microplastics' surfaces in water/sediment systems. *Toxics, 8*(3), 59. DOI: https://doi.org/10.3390/toxics8030059

Low, M. J. D. (1960). Kinetics of chemisorption of gases on solids. *Chemical Reviews, 60*(3), 267-312. DOI: https://doi.org/10.1021/cr60205a003

McLellan, M. T., Aber, D. J., Martin, M. E., Melillo, J. M., & Nadelhoffer, K. J. (1991). Determination of nitrogen, lignin, and cellulose content of decomposing leaf material by near infrared reflectance spectroscopy. *Canadian Journal of Forest Research, 21*(11), 1684-1688. DOI: https://doi.org/10.1139/x91-232

Merg, J. C., Rossett, F., Penha, F. G., Pergher, S. B. C., Petkowicz, D. I., & Santos, J. H. Z. (2010). Incorporação de dióxido de titânio em zeólitas para emprego em fotocatálise heterogênea. *Química Nova, 33*(7), 1525-1528. DOI: https://doi.org/10.1590/S0100-40422010000700019

Mittal, A., Mittal, J., & Kurup, L. (2006). Adsorption isotherms, kinetics and column operations for the removal of hazardous dye, Tartrazine from aqueous solutions using waste materials-Bottom Ash and De-Oiled Soya, as adsorbents. *Journal of Hazardous Materials, 136*(3), 567-578. DOI: https://doi.org/10.1016/j.jhazmat.2005.12.037

Moreno-Castilla, C., Ferro-García, M. A., Joly, J. P., Bautista-Toledo, I., Carrasco-Marín, F., & Rivera-Utrilla, J. (1995). Activated carbon surface modifications by nitric acid, hydrogen peroxide, and ammonium peroxydisulfate treatments. *Langmuir, 11*(11), 4386-4392. DOI: https://doi.org/10.1021/la00011a035

Mussatto, S. I., Dragone, G., & Roberto, I. C. (2006). Brewers' spent grain: generation, characteristics and potential applications. *Journal of Cereal Science, 43*(1), 1-14. DOI: https://doi.org/10.1016/j.jcs.2005.06.001

Mussatto, S. I., Fernandes, M., Rocha, G. J. M., Órfão, J. J. M., Teixeira, J. A., & Roberto, I. C. (2010). Production, characterization and application of activated carbon from brewer's spent grain lignin. *Bioresource Technology, 101*(7), 2450-2457. DOI: https://doi.org/10.1016/j.biortech.2009.11.025

Namane, A., Mekarzia, A., Benrachedi, K., Belhaneche-Bensemra, N., & Hellal, A. (2005). Determination of the adsorption capacity of activated carbon made from coffee grounds by chemical activation with $ZnCl_2$ and H_3PO_4. *Journal of Hazardous Materials, 119*(1-3), 189-194. DOI: https://doi.org/10.1016/j.jhazmat.2004.12.006

Nocente, F., Taddei, F., Galassi, E., & Gazza, L. (2019). Upcycling of brewers' spent grain by production of dry pasta with higher nutritional potential. *LWT*, *114*, 108421. DOI: https://doi.org/10.1016/j.lwt.2019.108421

Olsson, A.-M., & Salmén, L. (1997). The effect of lignin structure on the viscoelastic properties of wood. *Nordic Pulp and Paper Research Journal, 12*(3), 140-144. DOI: https://doi.org/10.3183/npprj-1997-12-03-p140-144

Patnukao, P., & Pavasant, P. (2008). Activated carbon from *Eucalyptus camaldulensis Dehn* bark using phosphoric acid activation. *Bioresource Technology, 99*(17), 8540-8543. DOI: https://doi.org/10.1016/j.biortech.2006.10.049

Pongkua, W., Dolphen, R., & Thiravetyan, P. (2019). Removal of gaseous methyl tert-butyl ether using bagasse activated carbon pretreated with chemical agents. *Journal of Chemical Technology and Biotechnology, 94*(5),1551-1558. DOI: https://doi.org/10.1002/jctb.5918

Ruthven, D. M. (1984). *Principles of adsorption and adsorption processes*. New York, NY: John Wiley & Sons.

Santa-Cruz, L. A., Soares, T. A. S., Galvão, R. A., Tavares, F. C., Araújo, I. R. M., Frizzo, C. P., ... Machado, G. (2021). Effect of heterocyclic nitrogen ionic liquid additives on the rate of backreaction in DSSCS: An electrochemical characterization. *Journal of Science: Advanced Materials and Devices, 6*(3), 483-487. DOI: https://doi.org/10.1016/j.jsamd.2021.05.007

Sganzerla, W. G., Ampese, L. C., Mussatto, S. I., & Forster-Carneiro, T. (2021b). A bibliometric analysis on potential uses of brewer's spent grains in a biorefinery for the circular economy transition of the beer industry. *Biofuels, Bioproducts and Biorefining, 15*(6), 1965-1988. DOI: https://doi.org/10.1002/bbb.2290

Sganzerla, W. G., Buller, L. S., Mussatto, S. I., & Forster-Carneiro, T. (2021c). Techno-economic assessment of bioenergy and fertilizer production by anaerobic digestion of brewer's spent grains in a biorefinery concept. *Journal of Cleaner Production, 297*, 126600. DOI: https://doi.org/10.1016/j.jclepro.2021.126600

Sganzerla, W. G., Zabot, G. L., Torres-Mayanga, P. C., Buller, L. S., Mussatto, S. I., & Forster-Carneiro, T. (2021a). Techno-economic assessment of subcritical water hydrolysis process for sugars production from brewer's spent grains. *Industrial Crops and Products, 171*,113836. DOI: https://doi.org/10.1016/j.indcrop.2021.113836

Silva, J. P., Sousa, S., Rodrigues, J., Antunes, H., Porter, J. J., Gonçalves, I., & Ferreira-Dias, S. (2004). Adsorption of acid orange 7 dye in aqueous solutions by spent brewery grains. *Separation and Purification Technology, 40*(3), 309-315. DOI: https://doi.org/10.1016/j.seppur.2004.03.010

Son, Y.-R., & Park, S.-J. (2020). Preparation and characterization of mesoporous activated carbons from nonporous hard carbon *via* enhanced steam activation strategy. *Materials Chemistry and Physics, 242*, 122454. DOI: https://doi.org/10.1016/j.matchemphys.2019.122454

Srihari, V., & Das, A. (2008). Comparative studies on adsorptive removal of phenol by three agro-based carbons: Equilibrium and isotherm studies. *Ecotoxicology and Environmental Safety, 71*(1), 274-283. DOI: https://doi.org/10.1016/j.ecoenv.2007.08.008

Taer, E., Apriwandi, A., Taslim, R., Malik, U., & Usman, Z. (2019). Single step carbonization-activation of durian shells for producing activated carbon monolith electrodes. *International Journal of Electrochemical Science, 14*, 1318-1330. DOI: https://doi.org/10.20964/2019.02.67

Vanreppelen, K., Vanderheyden, S., Kuppens, T., Schreurs, S., Yperman, J., & Carleer, R. (2014). Activated carbon from pyrolysis of brewer's spent grain: Production and adsorption properties. *Waste Management & Research, 32*(7), 634-645. DOI: https://doi.org/10.1177/0734242x14538306

Vasques, A. R., Souza, S. M. A. G. U., Weissenberg, L., Souza, A. A. U., & Valle, J. A. B. (2011). Adsorção dos corantes RO16, RR2 e RR141 utilizando lodo residual da indústria têxtil. *Engenharia Sanitária e Ambiental, 16*(3), 245-252. DOI: https://doi.org/10.1590/S1413-41522011000300007

Xiaobo, Z., Jiewen, Z., Povey, M. J. W., Holmes, M., & Hanpin, M. (2010). Variables selection methods in near-infrared spectroscopy. *Analytica Chimica Acta, 667*(1-2), 14-32. DOI: https://doi.org/10.1016/j.aca.2010.03.048

Zhang, J., & Wang, Q. (2016). Sustainable mechanisms of biochar derived from brewers' spent grain and sewage sludge for ammonia–nitrogen capture. *Journal Of Cleaner Production, 112*(Part 5), 3927-3934. DOI: https://doi.org/10.1016/j.jclepro.2015.07.096